②

POR-2215(EX)
(WT-2215)(EX)
EXTRACTED VERSION

OPERATION SUNBEAM, SHOT SMALL BOY

Project Officer's Report—Project 2.9

Fallout Collection and Gross Sample Analysis

J. D. Sartor
W. B. Lane
U. S. Naval Radiological Defense Laboratory
San Francisco, CA

K. H. Larson
Laboratory of Nuclear Medicine and Radiation Biology
University of California at Los Angeles
Los Angeles, CA

23 October 1964

NOTICE:
This is an extract of POR-2215 (WT-2215), Operation SUNBEAM, Project 2.9.

Extracted version prepared for
Director
DEFENSE NUCLEAR AGENCY
Washington, DC 20305-1000

1 September 1985

OPERATION SUN BEAM

SHOT SMALL BOY

PROJECT OFFICERS REPORT—PROJECT 2.9

FALLOUT COLLECTION AND GROSS SAMPLE ANALYSIS

P. D. LaRiviere, Project Officer
J. D. Sartor
W. B. Lane

U. S. Naval Radiological Defense Laboratory
San Francisco 24, California

K. H. Larson

Laboratory of Nuclear Medicine and Radiation Biology
University of California at Los Angeles
Los Angeles 54, California

ABSTRACT

The objectives of this project were: (a) to make quantitative collections of fallout in order to determine mass per unit area, ionization decay rate and gamma ray spectra, size-activity distribution, size distribution versus time of deposit: to perform limited leaching studies; to assess the relative amounts of short-lived induced products in the fallout; and to provide Project 2.10 (Physicochemical and Radiochemical Analysis) with gross and size-separated fallout samples for further physical, chemical, and radiochemical analyses. (b) To measure, during fallout, the deposition dynamics of arrival time, mass deposition rate, and time of cessation. (c) To determine the size distribution and concentration of airborne fallout debris as a function of time after burst, and to measure the amount and size distribution of that fraction penetrating test ventilation intake configurations. (d) To estimate visibility, near ground level, in the dust cloud produced by blast and shock.

To satisfy these objectives 6 manned fallout stations and 73 other collection stations were established in Frenchman Flat; 24 stations were installed in the Indian Springs Valley (18 miles east of ground zero); and 247 points were instrumented for fallout collection by mobile field teams directed across the predicted path of the fallout by radio and telephone. Most of the closer stations were instrumented with gamma intensity versus time recorders fielded by Project 2.11. Complete analytical facilities for gross fallout analysis were set up at the Nevada Test Site (NTS).

The fallout was well-placed through the close-in array, with 3 out of 6 manned stations receiving significant amounts; of the other 73 Frenchman Flat stations, 40 were within the 10 mr/hr at 1-hour line, and in Indian Springs Valley, measureable amounts of fallout were deposited at 15 of the 24 stations. Of the 247 off-site stations established, 97 were contaminated with fallout debris.

The quality and kinds of measurements made on this operation were considerably improved over previous weapon test field work as a result of the experience gained by project personnel over the years prior to the moratorium. Sufficient data were obtained to satisfy most of the project objectives.

Crater dimensions were determined by aerial photography. The crater was merely a shallow irregular indentation in the playa with no characteristic lip. It is evident that the term surface burst only loosely describes this event.

The particle size and gamma activity distribution data reported have not been examined and interpreted. It appears, however, that active fallout particles were formed which were larger than the native soil particles originally present in the vicinity of ground zero. In this respect, the close-in Small Boy fallout superficially resembled that from Operation Jangle S shot more than Frenchman Flat soil.

Na^{24} was the only induced gamma activity noticeable in the measurements of this project. There appeared to be little relative fractionation of gamma-emitting nuclides from station to station, because the decay curves were very much alike. The slopes of the field decay curves measured with the NRDL Project 2.11 gamma intensity-time recorders also showed little spread, averaging about $t^{-1.3}$.

Measurements made on fallout samples exposed o air showed a continuing loss of iodine over a period of 12 days following the burst. The fraction of activity associated

Planning estimates of fallout mass per unit area, particle size range at a given location, and 1-hour gamma ionization rates along the downwind axis of the pattern were based on a pre-publication version of a simplified fallout model described in Reference 6. The NRDL D Fallout Model (Reference 7) was used with an actual acceptable NTS wind structure to yield standard intensities (r/hr at 1 hour for the complete deposit, measured 3 feet above the ground) at each of the station locations. These typical values in turn became the controlling factors in planning shelter withdrawal and sample recovery times and routes. A maximum allowable dose of 3.0 r for the operation was assumed.

It was recognized that the predictions of both models mentioned were based on particle size-activity distributions associated with Jangle S-like soils. In contrast, however, the Frenchman Flat ground zero soil, to a depth of at least 30 feet in the vicinity of zero, contained virtually no particles > 150 microns in diameter; therefore, any large particles found in the fallout would have to have been formed by aggregation, sintering of small particles, or freezing of drops derived from molten soil. Whether the Small Boy fallout particle size distributions would resemble those of Jangle S or the fine material of the shot environment was a point of major uncertainty.

Since the molten volume must be small compared to the total crater volume, it appeared that a sizeable fraction of the total activity would condense on the large available surface presented by the physically unaltered fine particles. In this event, the fallout would extend many miles downwind in larger amounts than estimated, and the close-in fallout would be correspondingly depleted. For recovery planning then, a model pattern such as shown in Figure 2.1 resulted in conservative dose estimates.

2.2 INSTRUMENTATION

2.2.1 Collector Rationale. Many of the project objectives could not have been met unless the samples collected were representative, in the manner desired, of the deposit at the location at which they were collected. Three approaches in collector design were used here:

1. The granular collector, for which the geometry (essentially flush with the ground) and collecting surface characteristics simulated natural terrain. Another example of this type was the buried collector, filled with soil and buried flush with the ground surface, so that the collecting area was indistinguishable from the surrounding terrain. This type of collector partakes in any redistribution of material, due to wind and weather, that may take place after fallout deposition;

3.1 SHOT CONDITIONS AND METEOROLOGY

3.1.1 Device Information. The Small Boy shot was fired 14 July 1962 at 1130:123 PDT in Frenchman Flat, NTS, at Nevada State Coordinates N747, 907.43, E717, 118.39, ground elevation 3,078 feet above MSL. The

employed for this event was mounted on a wooden tower with the device center of gravity 10 feet above the surface of the ground. The yield was These data, atmospheric conditions, and some burst height scaling factors may be found in Reference 19.

bare collectors, and the greased collectors at each station. It is seen that in all cases except at Stations 101, 200, and 303, the mean value for the greased collector was comparable to the bare collectors. Generally however, the mean gamma activity value for the greased collectors was slightly higher.

3.7.2 Radioiodine Study. Iodine loss by air exposure is reported in Table 3.20. The progressive decrease in the observed iodine/total fraction with time indicates a loss of iodine during the period of air exposure.

Reference 20 shows that at 13 days the radioisotopes of iodine contribute 20.3 percent of the gamma radiation (by 4π ionization chamber) from normal U^{235} thermal fission products. Dividing the observed iodine/total fractions by the expected fraction yields the percentage of the theoretical iodine actually recovered. The most apparent reason for the low initial percentage was the inability of the analytical procedure to remove iodine which might have been trapped within insoluble particles. In addition, the iodine may have been depleted from the outset due to fractionation during the fallout formation process.

It is emphasized that these results were obtained by an analytical procedure which was developed in the field. Although duplicates were consistent, the iodine recovery is not known for this method, nor was the purity of the iodine product, since no spectra or decays were obtained; however, spectra from a Project Sedan sample which was processed in a similar manner showed a very high radioiodine purity.

TABLE 3.1 WIND VELOCITY FROM OBSERVATIONS OF U.S. WEATHER BUREAU, FRENCHMAN FLAT AREA STATION

Time of Observ. PDT	Altitude Above Frenchman Flat feet: Surface	4000	5000	6000	7000	8000	9000	10000	12000	14000	16000	18000	20000
	degrees/knots												
0720	Calm	020/07	020/07	030/07	060/05		270/04	290/06	300/08	290/08	280/14	280/14	280/23
0750	Calm	350/05	030/07	060/06	070/06		280/08	300/08	290/10	280/08	240/10	280/12	290/26
0800*	050/05	310/05	240/05	240/05	240/05	250/10	260/10	260/10	270/15	280/15	290/15	290/15	300/20
0830	Calm	360/04	020/06	060/06	060/04		280/06	270/08	290/08	270/08	250/07	290/23	-
0900	115/01	340/04	030/05	090/03	100/02	270/04							
0940	-	040/02	070/04	100/04	140/02	190/01	290/04	300/07	280/11	290/10	250/11	240/09	
0950	Calm	050/03	090/02	100/02		280/03	270/03	270/08	260/06	250/07	250/07	250/07	280/10
1030	Calm	130/01	125/02	030/02	330/02	275/03	270/06	236/12	250/08	250/08	240/16	270/11	290/21
1045	Calm	Calm		203/03	270/02	262/05	234/06	233/11	250/08	250/09	240/06	270/08	290/16
1100		300/01	310/01	330/02	280/02	250/06	240/12	240/16	240/08	240/08	240/08	280/14	280/25
1145		145/04	167/05	176/06	168/06	185/03	233/05	243/11	235/09	229/08	228/07	260/13	285/23
1405		200/08	190/10	-	200/14	200/14	200/14	200/13	220/11	250/08	250/09	270/14	
1432	220/05	240/06	230/07	230/08	230/07	210/10	220/12	230/12	250/10	240/08	250/10	260/13	270/18

*Forecast from 0200 soundings.

TABLE 3.20 LOSS OF IODINE FROM PARTICULATE DEBRIS BY AIR EXPOSURE

Sample #	Weight	Duration of Air Exposure*	4 π Activity at 13d		Observed	Observed I / Expected I**
	(g)	(d)	Total (ma)	Iodine (ma)	Iodine/Total	%
S2PC8	1.990	2	138×10^{-8}	960×10^{-10}	0.0696	34.3
S5PC8	0.471	2	880×10^{-9}	700×10^{-10}	0.0796	39.2
S2PC11	1.260	6	664×10^{-9}	330×10^{-10}	0.0495	24.4
S5PC11	0.206	6	100×10^{-8}	550×10^{-10}	0.0550	27.1
S2PC19	0.962	12	430×10^{-9}	108×10^{-10}	0.0251	12.4
S5PC19	0.399	12	870×10^{-9}	265×10^{-10}	0.0305	15.0

* Measured from detonation time.

** Reference 20, at D + 13d $\frac{\text{I (ma)}}{\text{fission product (ma)}} = 0.203$ expected.

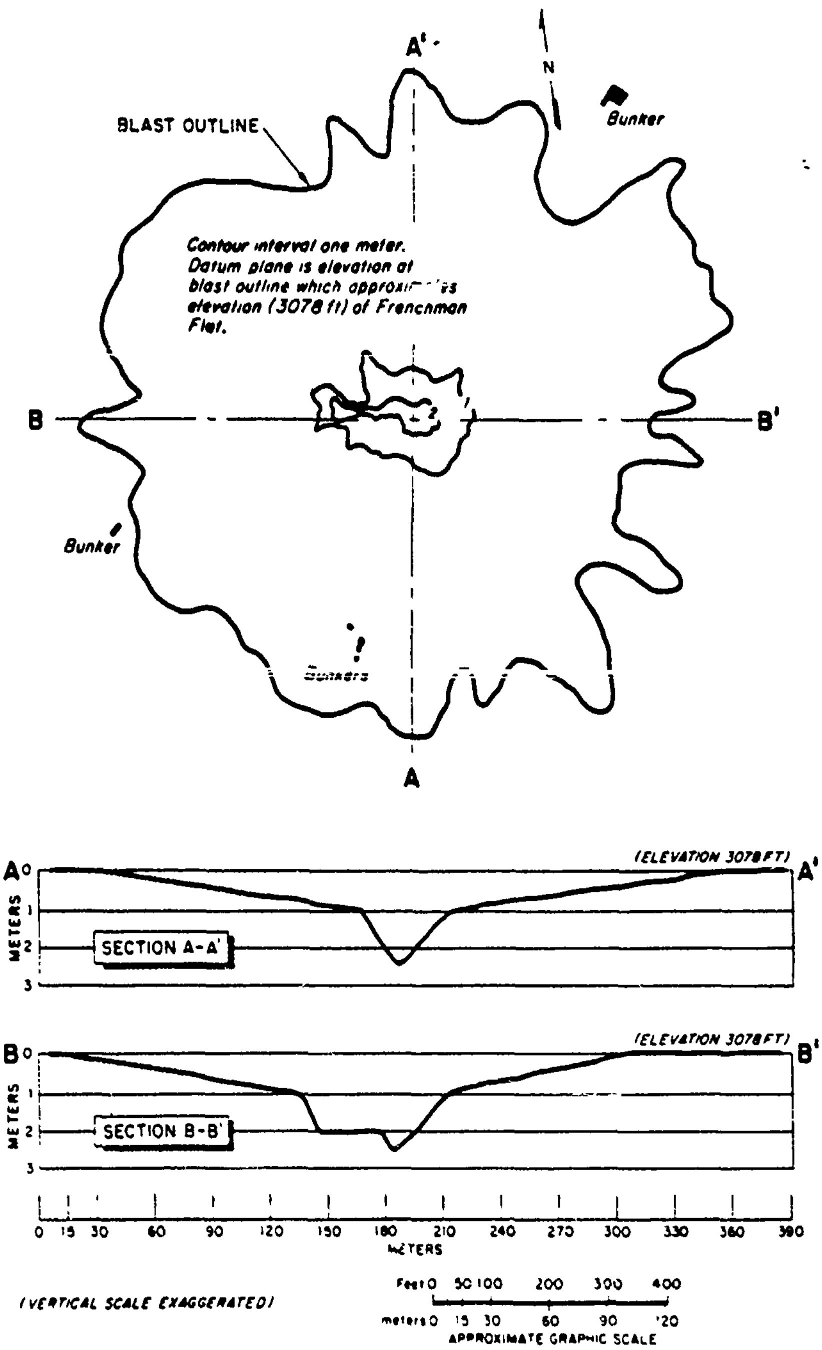

Figure 3.2 Crater contours and profiles.

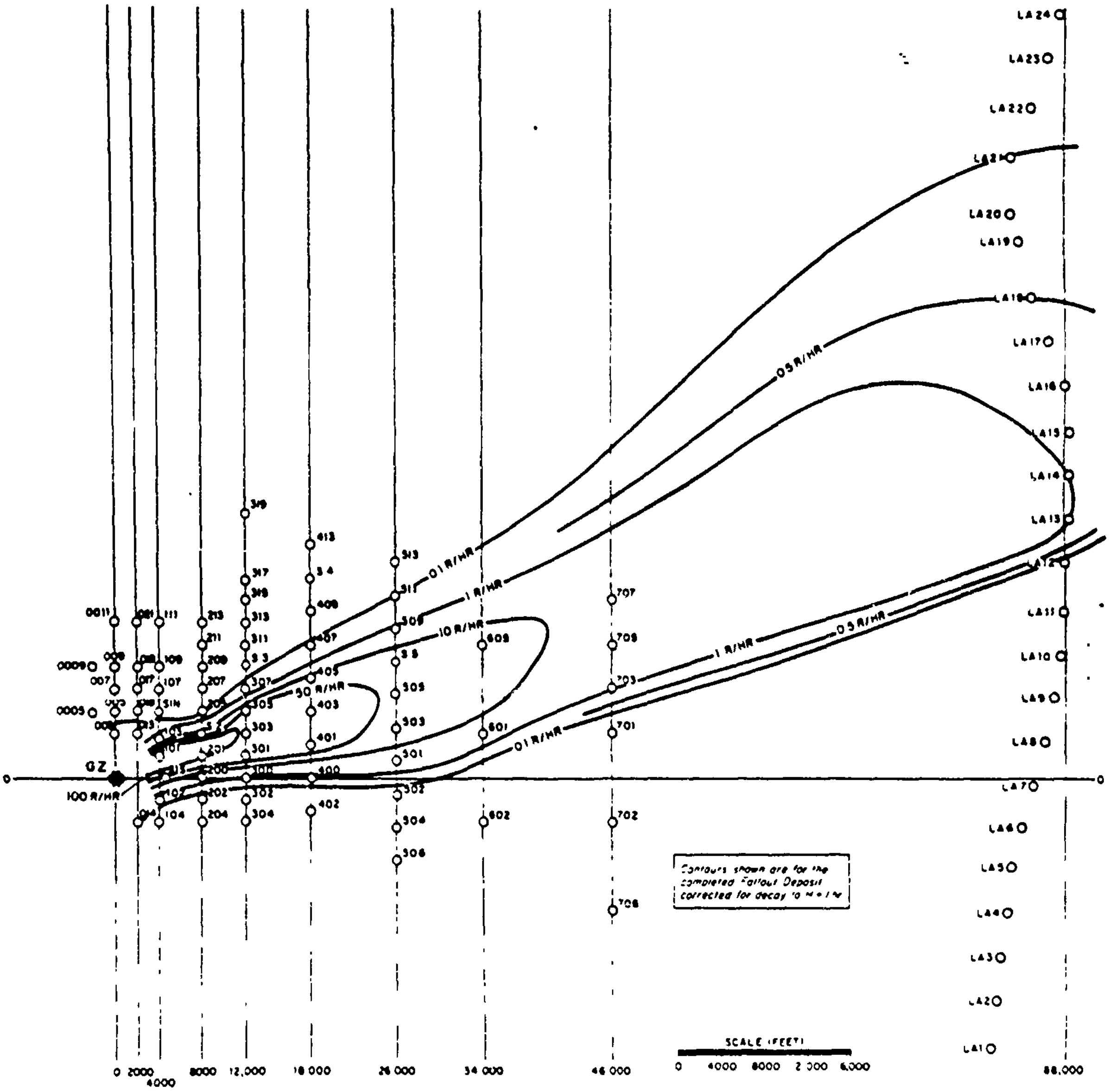

Figure 3.4 Fallout path through Project 2.9 and 2.11 arrays, Frenchman Flat and Indian Springs Valley.

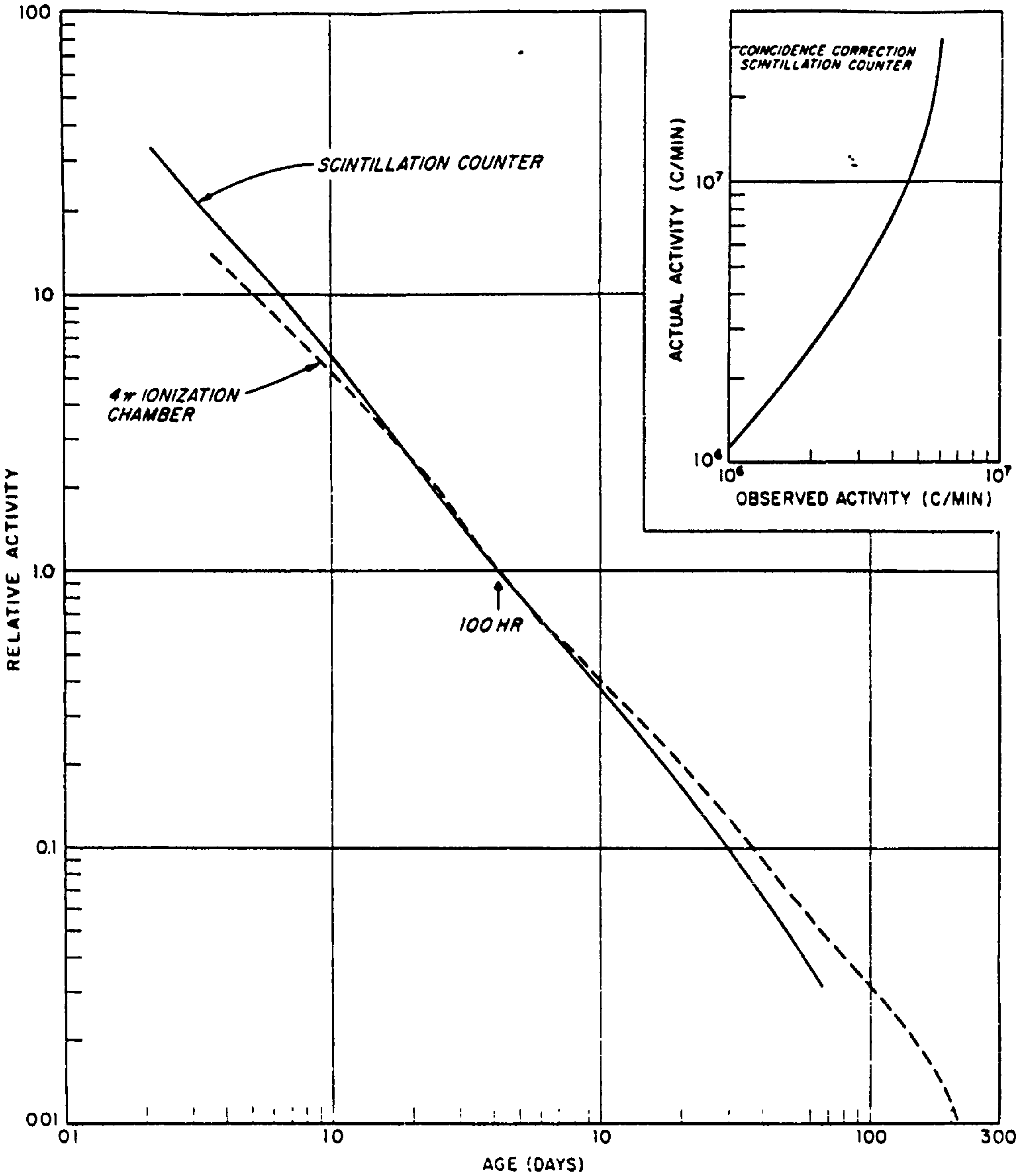

Figure 3.6 Representative sample gamma decay rates by low-geometry scintillation counter and 4π ionization chamber; coincidence correction curve for the scintillation counter.

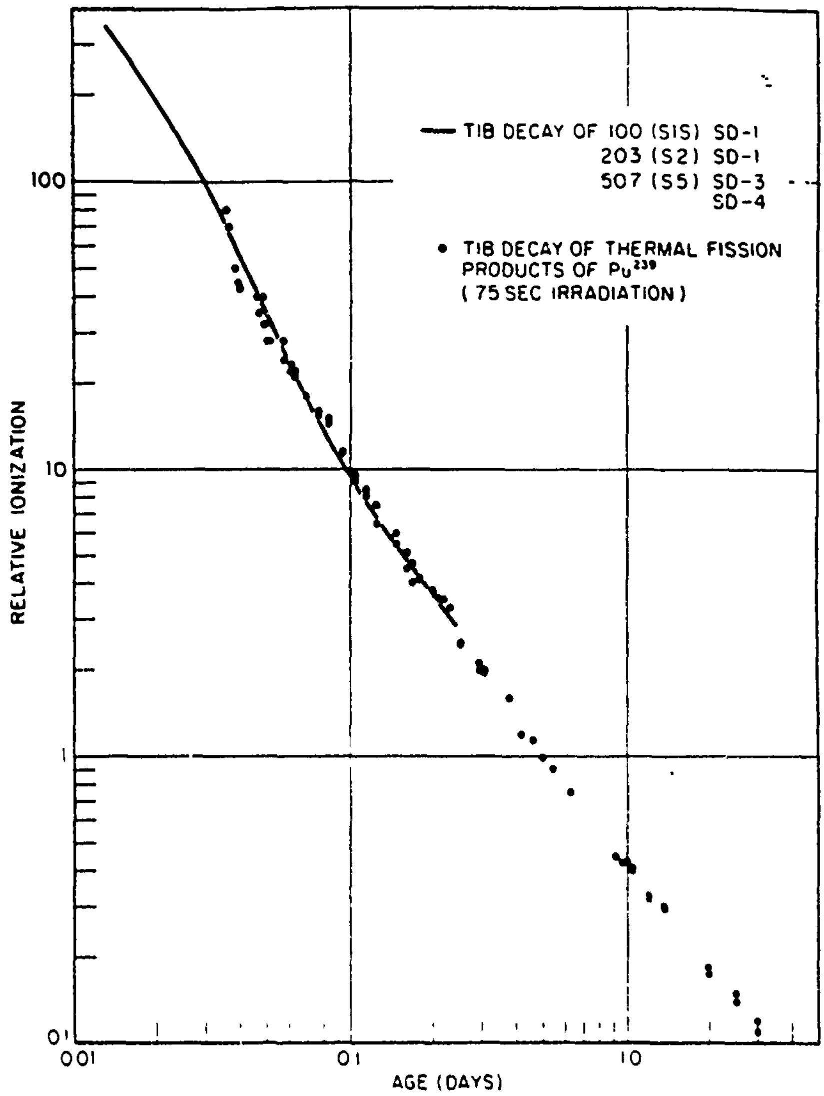

Figure 3.7 T1B decay of SD and plutonium fission product samples.

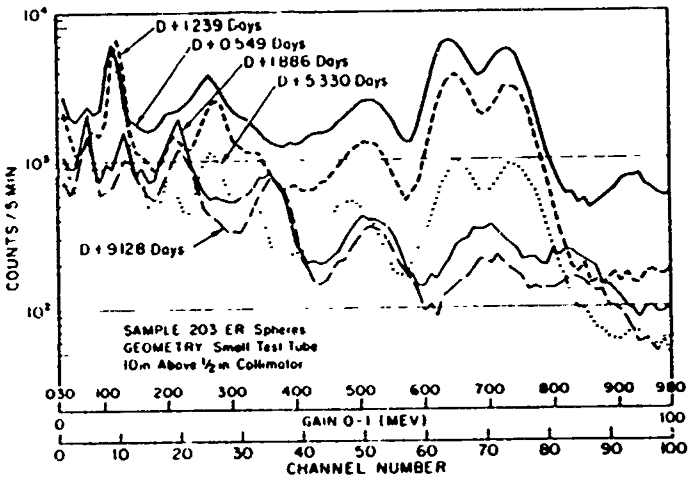

Figure 3.8 Effect of decay on pulse height distributions of activity in fused spheres.

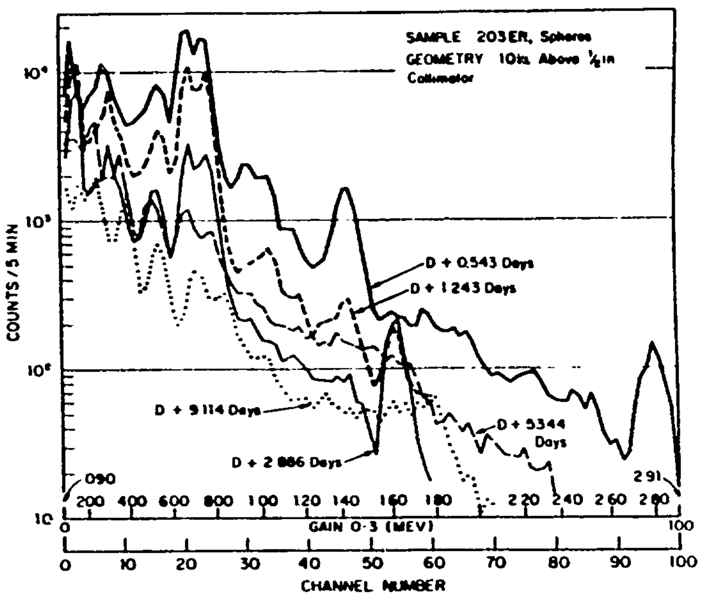

Figure 3.9 Effect of decay on pulse height distributions of activity in fused spheres.

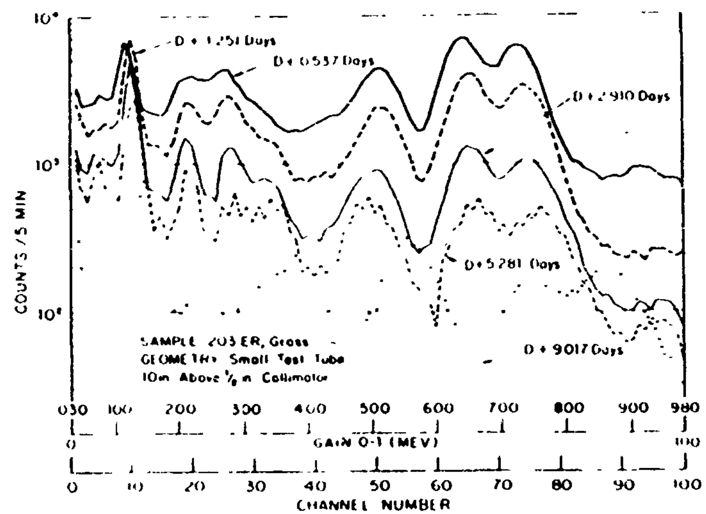

Figure 3.10 Effect of decay on pulse height distributions of activity in gross collections.

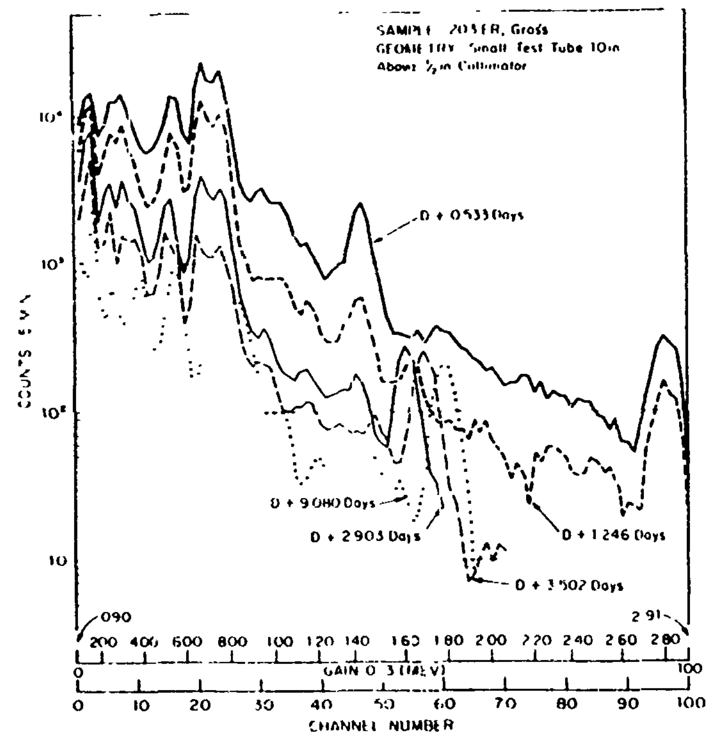

Figure 3.11 Effect of decay on pulse height distributions of activity in gross collections.

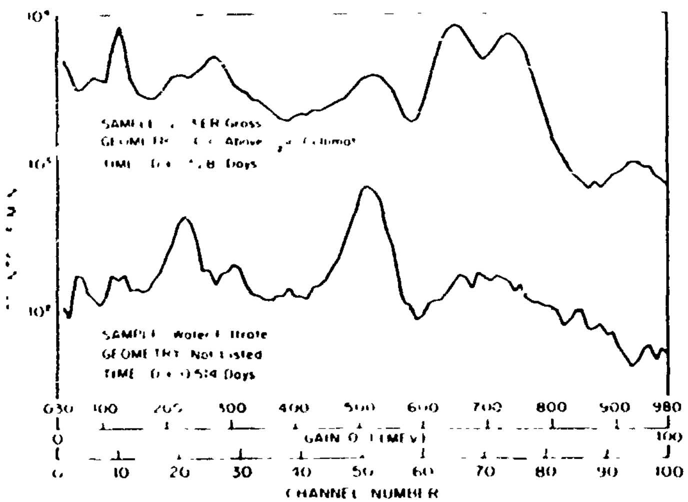

Figure 3.12 Pulse height distributions of activity.

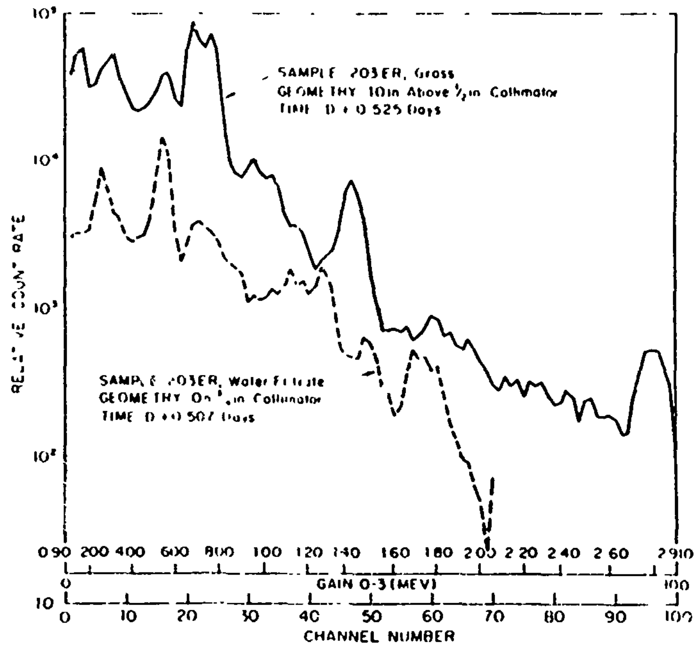

Figure 3.13 Pulse height distributions of activity.

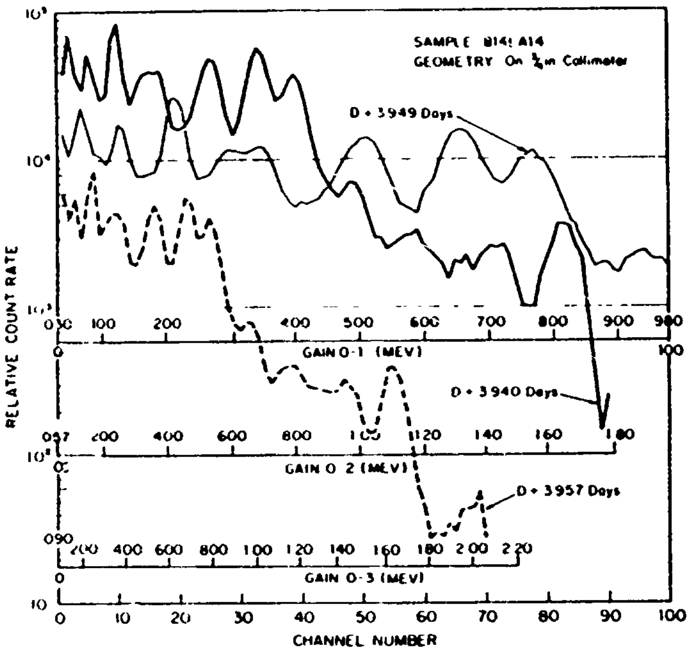

Figure 3.14 Pulse height distributions of activity removed by xylene wash.

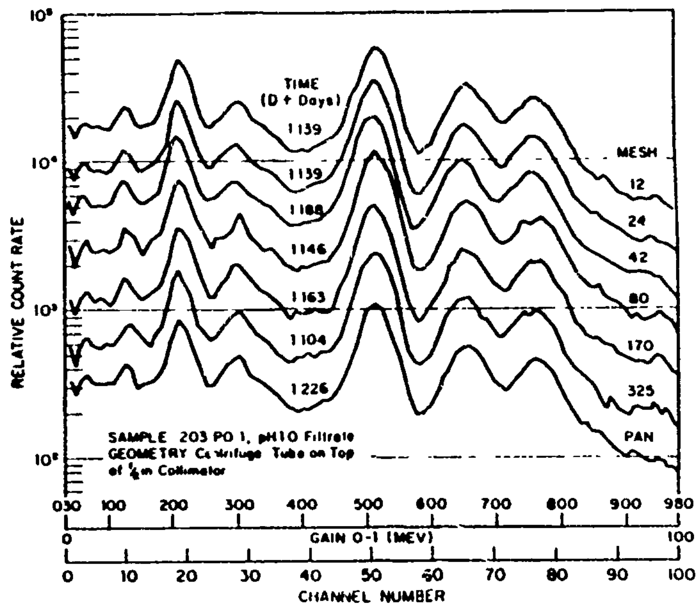

Figure 3.15 Pulse height distributions of leached activity.

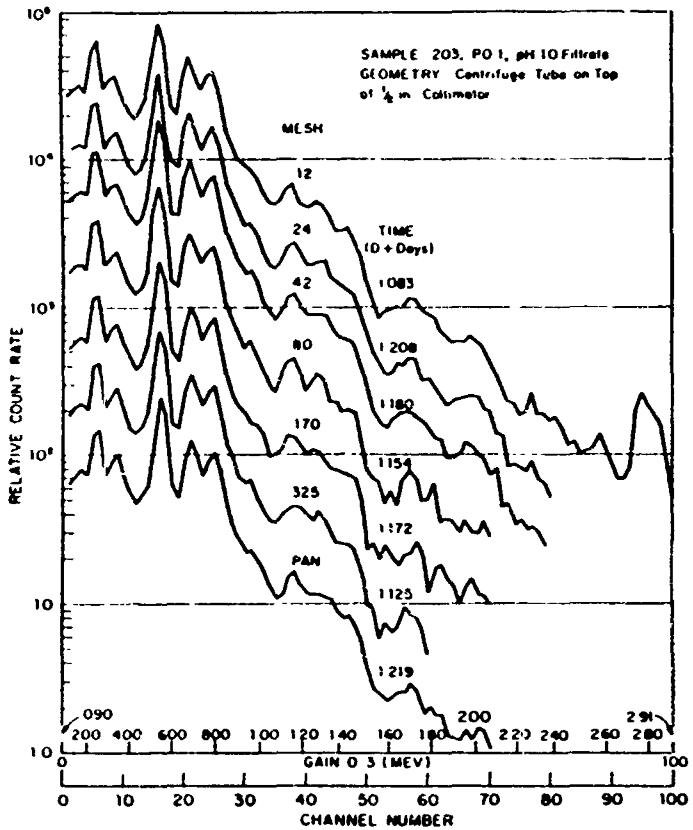

Figure 3.16 Pulse height distributions of leached activity.

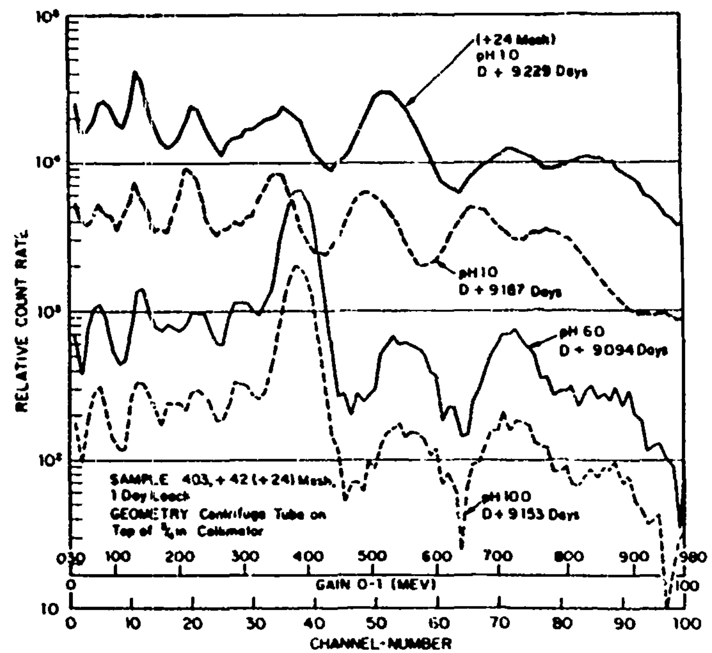

Figure 3.17 Pulse height distributions of leached activity.

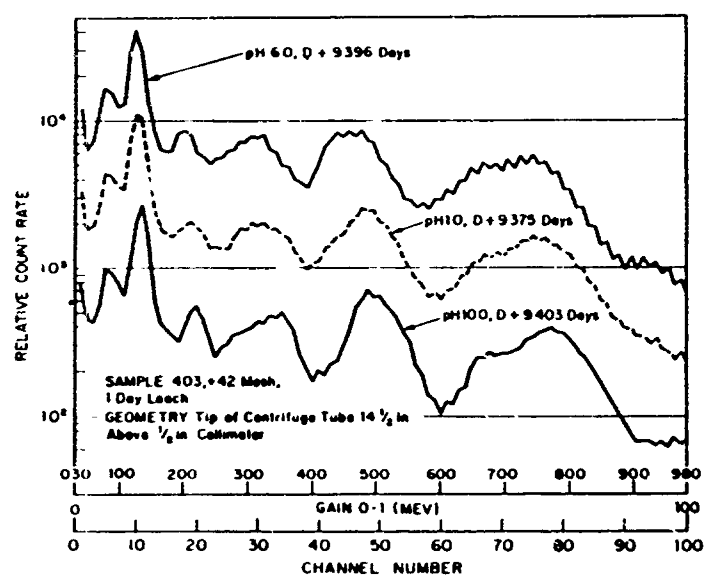

Figure 3.18 Pulse height distributions of residual activity after leaching.

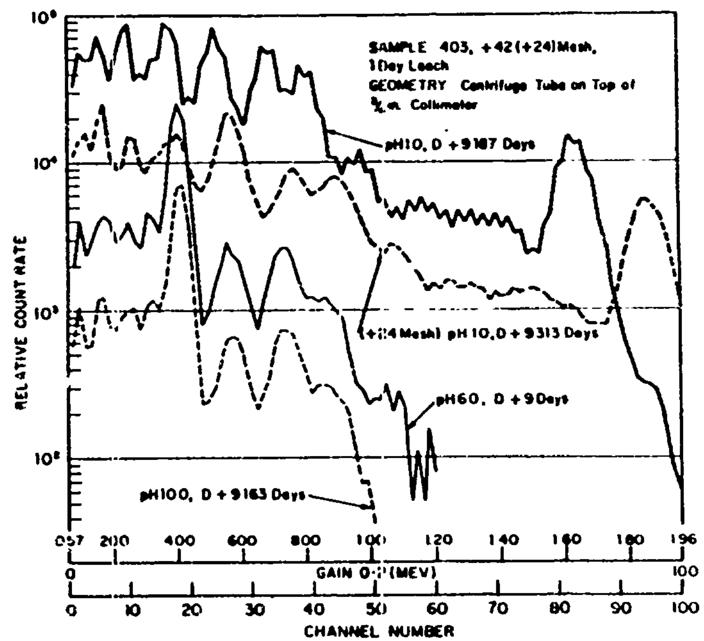

Figure 3.19 Pulse height distributions of leached activity.

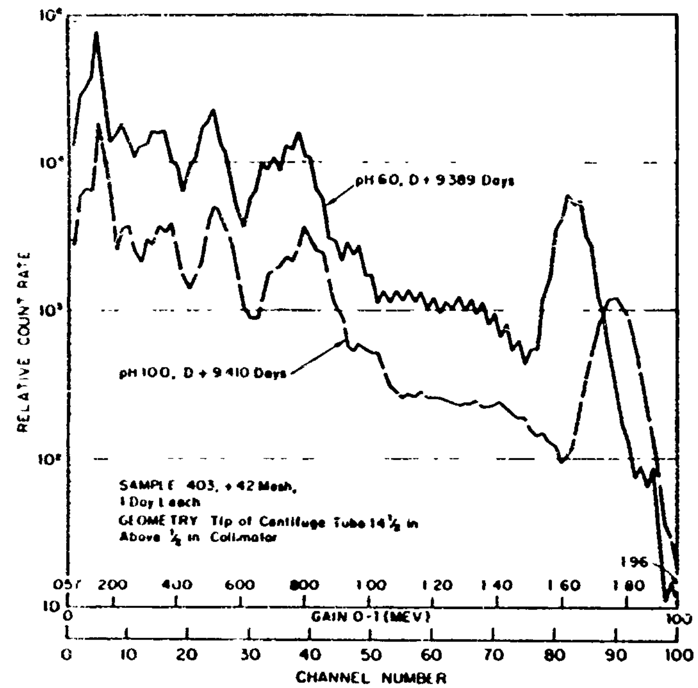

Figure 3.20 Pulse height distributions of residual activity after leaching.

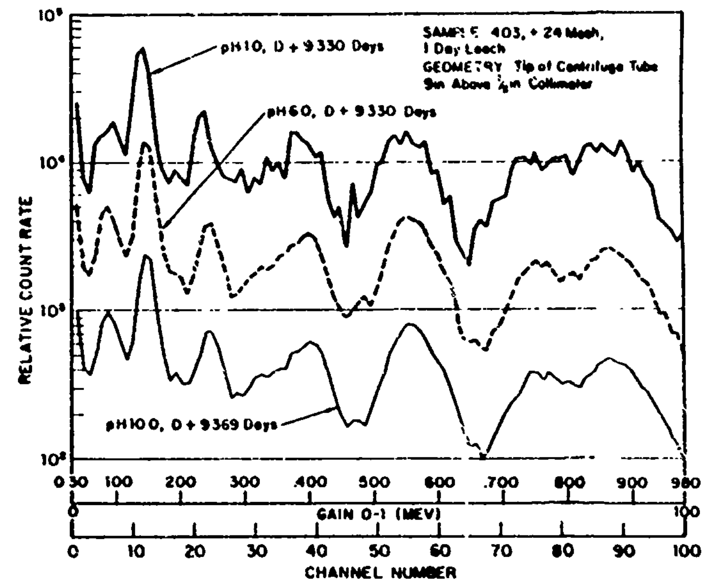

Figure 3.21 Pulse height distributions of residual activity after leaching.

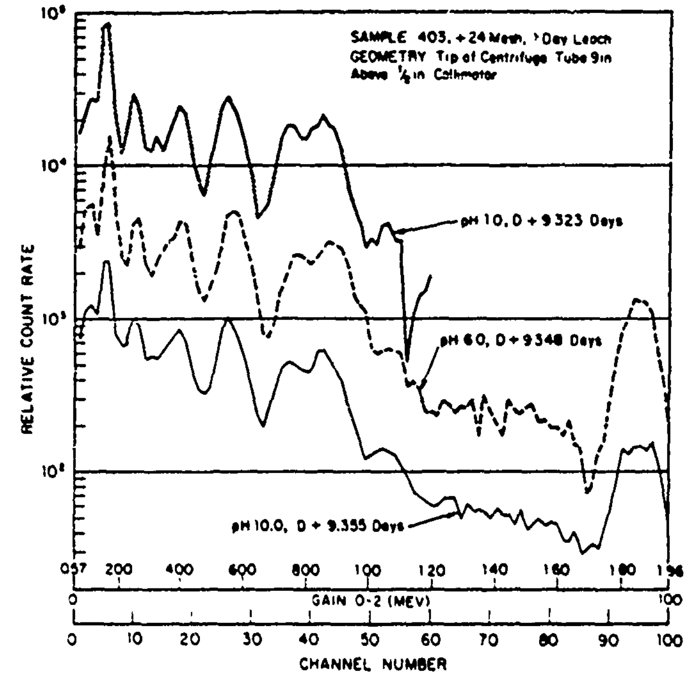

Figure 3.22 Pulse height distributions of residual activity after leaching.